

AD-A175 540

THE INFLUENCE OF BUBBLES ON SEA SURFACE BACKSCATTER
MEASUREMENTS (DER EIN. (U) NAVAL UNDERWATER SYSTEMS
CENTER NEWPORT RI P D KOENIGS ET AL. 26 OCT 86

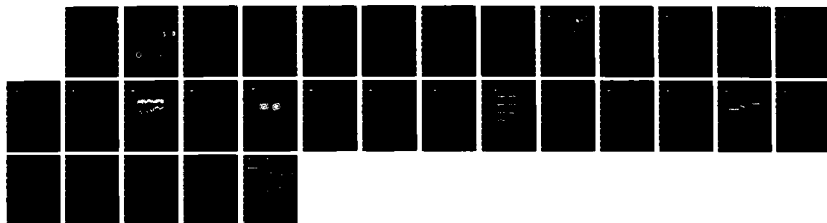
1/1

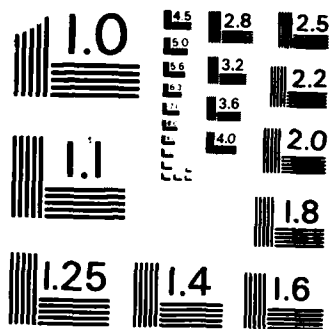
UNCLASSIFIED

NUSC-TD-7811

F/G 17/1

NL





MICROCOPY RESOLUTION TEST CHART
NATIONAL BUREAU OF STANDARDS-1963-A

12

AD-A175 540

The Influence of Bubbles on Sea Surface Backscatter Measurements

Der Einfluss von Blasen auf die Messung der Rückstreuungseigenschaften der Meeresoberfläche

**A Paper to be Presented at the
Colloquium on Acoustics in Torpedo Technology,
Newport, Rhode Island**

**DTIC
ELECTE
DEC 3 1 1986
S D D**

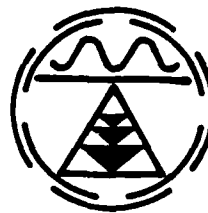
**Paul D. Koenigs
Joseph M. Monti**
*Surface Ship Sonar Department
Naval Underwater Systems Center*

**Bernd Nützel
Heinz Herwig**
*Forschungsanstalt der Bundeswehr
für Wasserschall- und Geophysik*

26 October 1986



NAVAL UNDERWATER SYSTEMS CENTER
Newport, Rhode Island • New London, Connecticut



**FORSCHUNGSANSTALT DER BUNDESWEHR
FÜR WASSERSCHALL- UND GEOPHYSIK**
Kiel

DTIC FILE COPY

Approved for public release; distribution unlimited.

Preface

This document describes work performed under Data Exchange Agreement MWDDEA-N-67-G-4207, Subproject 2, between the Forschungsanstalt der Bundeswehr fuer Wasserschall- und Geophysik (FWG), Kiel, Federal Republic of Germany (FRG), and the Naval Underwater Systems Center (NUSC), New London, Connecticut, USA. The U.S. effort was accomplished under NUSC Project No. B68201, "Environmental Dependence of Acoustic Surface Scatter," Principal Investigator, P. D. Koenigs (NUSC Code 3331). Funding was provided under Program Element 62759N, by Naval Sea Systems Command (NAVSEA 63R); Dr. R. Farwell (NORDA 113), Manager, and by NUSC Associate Technical Director, Research and Technology Office. The work was performed under the auspices of the Office of the Chief of Naval Research (Code 122).

Vorwort

Die Messungen an der Forschungsplattform NORDSEE wurden im Rahmen des Datenaustauschabkommens MWDDEA-N-67-G-4207, Subproject 2, durchgeführt. Die Abstimmung des jährlichen Forschungsprogrammes der FWG mit dem Inhalt des DEA erfolgte durch RüFo 3 des BMVg der Bundesrepublik Deutschland.

APPROVED: 26 October 1986



L. Freeman
Surface Ship Sonar Department
Naval Underwater Systems Center

EINVERSTANDEN: 26 Oktober 1986



PROF. Dr. G. Ziehm
Director, Defence Research Institute
for Underwater Sound and Geophysics
Federal Republic of Germany

The Influence of Bubbles on Sea Surface Backscatter Measurements

Der Einfluss von Blasen auf die Messung der Rückstreuungseigenschaften der Meeresoberfläche

**A Paper to be Presented at the
Colloquium on Acoustics in Torpedo Technology,
Newport, Rhode Island**

**Paul D. Koenigs
Joseph M. Monti
*Surface Ship Sonar Department
Naval Underwater Systems Center***

**Bernd Nützel
Heinz Herwig
*Forschungsanstalt der Bundeswehr
für Wasserschall- und Geophysik***

**This report is the result of a cooperative research project conducted under the auspices of ONR's
data exchange agreement MWDDEA-N-67-G-4207, Subproject 2.**

APPROVED: 26 October 1986

EINVERSTANDEN: 26 Oktober 1986



**Dr. William A. Von Winkle
Naval Underwater Systems Center
for the United States Project Officer**



**BDir Harry Kerbs
German Project Officer
MOD Bonn, Code Rü V4**

UNCLASSIFIED

SECURITY CLASSIFICATION OF THIS PAGE

ADA175540

REPORT DOCUMENTATION PAGE

1a. REPORT SECURITY CLASSIFICATION UNCLASSIFIED			1b. RESTRICTIVE MARKINGS		
2a. SECURITY CLASSIFICATION AUTHORITY			3. DISTRIBUTION/AVAILABILITY OF REPORT		
2b. DECLASSIFICATION/DOWNGRADING SCHEDULE			Approved for public release; distribution unlimited.		
4. PERFORMING ORGANIZATION REPORT NUMBER(S) NUSC TD 7811			5. MONITORING ORGANIZATION REPORT NUMBER(S)		
6a. NAME OF PERFORMING ORGANIZATION Naval Underwater Systems Center		6b. OFFICE SYMBOL (If applicable) 3331		7a. NAME OF MONITORING ORGANIZATION	
6c. ADDRESS (City, State, and ZIP Code). New London Laboratory New London, CT 06320		7b. ADDRESS (City, State, and ZIP Code)			
8a. NAME OF FUNDING/SPONSORING ORGANIZATION Office of Naval Research		8b. OFFICE SYMBOL (If applicable) 102D		9. PROCUREMENT INSTRUMENT IDENTIFICATION NUMBER	
8c. ADDRESS (City, State, and ZIP Code) Arlington, VA 22217		10. SOURCE OF FUNDING NUMBERS			
		PROGRAM ELEMENT NO.		PROJECT NO. B68201	WORK UNIT ACCESSION NO.
11. TITLE (Include Security Classification) THE INFLUENCE OF BUBBLES ON SEA SURFACE BACKSCATTER MEASUREMENTS					
12. PERSONAL AUTHOR(S) P. Koenigs and J. Monti (NUSC); B. Nützel and H. Herwig (FWG)					
13a. TYPE OF REPORT		13b. TIME COVERED FROM TO		14. DATE OF REPORT (Year, Month, Day) 1986 October 26	
				15. PAGE COUNT 22	
16. SUPPLEMENTARY NOTATION A paper presented at a Colloquium on Acoustics in Torpedo Technology					
17. COSATI CODES			18. SUBJECT TERMS (Continue on reverse if necessary and identify by block number)		
FIELD	GROUP	SUB-GROUP	Acoustic Scattering Strength; Frequency Dependence; Backward Surface Scatter Grazing Angle Dependence; Bubbles High Resolution		
19. ABSTRACT (Continue on reverse if necessary and identify by block number)					
<p>The results from a recent sea surface acoustic scattering experiment, which was conducted in the North Sea, are presented with accompanying sea surface roughness parameters and subsurface bubble information. The acoustic data were obtained utilizing a high resolution (narrow beamwidth) pulsed parametric sonar transmitter and conventional receiver. Scattering strength values were obtained as a function of frequency (3-18 kHz) for wind speeds from 2 to 45 knots. It appears that the backscattering</p>			<p>Im Rahmen eines Datenaustauschabkommens zwischen den Vereinigten Staaten und der Bundesrepublik Deutschland wurden im Herbst 1985 an der Forschungsplattform "NORDSEE" Untersuchungen zu den akustischen Streueigenschaften der Meeresoberfläche durchgeführt. Die Ergebnisse dieses Experimentes werden gemeinsam mit den Seegangsparemtern dargestellt.</p> <p>Als Schallquelle diente ein parametrischer Wandler hoher Richtwirkung, der im kon-</p>		
20. DISTRIBUTION/AVAILABILITY OF ABSTRACT <input type="checkbox"/> UNCLASSIFIED/UNLIMITED <input checked="" type="checkbox"/> SAME AS RPT. <input type="checkbox"/> DTIC USERS			21. ABSTRACT SECURITY CLASSIFICATION UNCLASSIFIED		
22a. NAME OF RESPONSIBLE INDIVIDUAL Paul D. Koenigs			22b. TELEPHONE (Include Area Code) (203)440-4835		22c. OFFICE SYMBOL 3331

18. (Cont'd)

NORDSEE Research Platform
 North Sea
 Parametric Sonar;
 Radar Backscatter;

roughness dependence;
 Shallow Water;
 Wave Height Dependence;
 Wind Dependence;

19. (Cont'd)

Strength at a 30° grazing angle is caused by the high frequency wavenumber spectrum at low wind speeds and by sub-surface bubbles at high wind speeds. The backscattering strength shows strong fluctuations in the intermediate region caused by both scattering mechanisms.

ventionellen Betrieb als Empfänger arbeitete. Rückstreustärken wurden in Abhängigkeit der Frequenz (3 bis 18 kHz) für Windgeschwindigkeiten von 2 bis 45 Knoten gemessen. Der Bericht zeigt, dass die Rückstreustärke bei einem Glanzwinkel von 30° bei geringen Windgeschwindigkeiten vom hoch frequenten Seegangsspektrum und bei hohen Windgeschwindigkeiten von Blasen bestimmt wird. Im Zwischenbereich weist die Rückstreustärke starke Fluktuationen auf, die von beiden Streumechanismen verursacht werden.

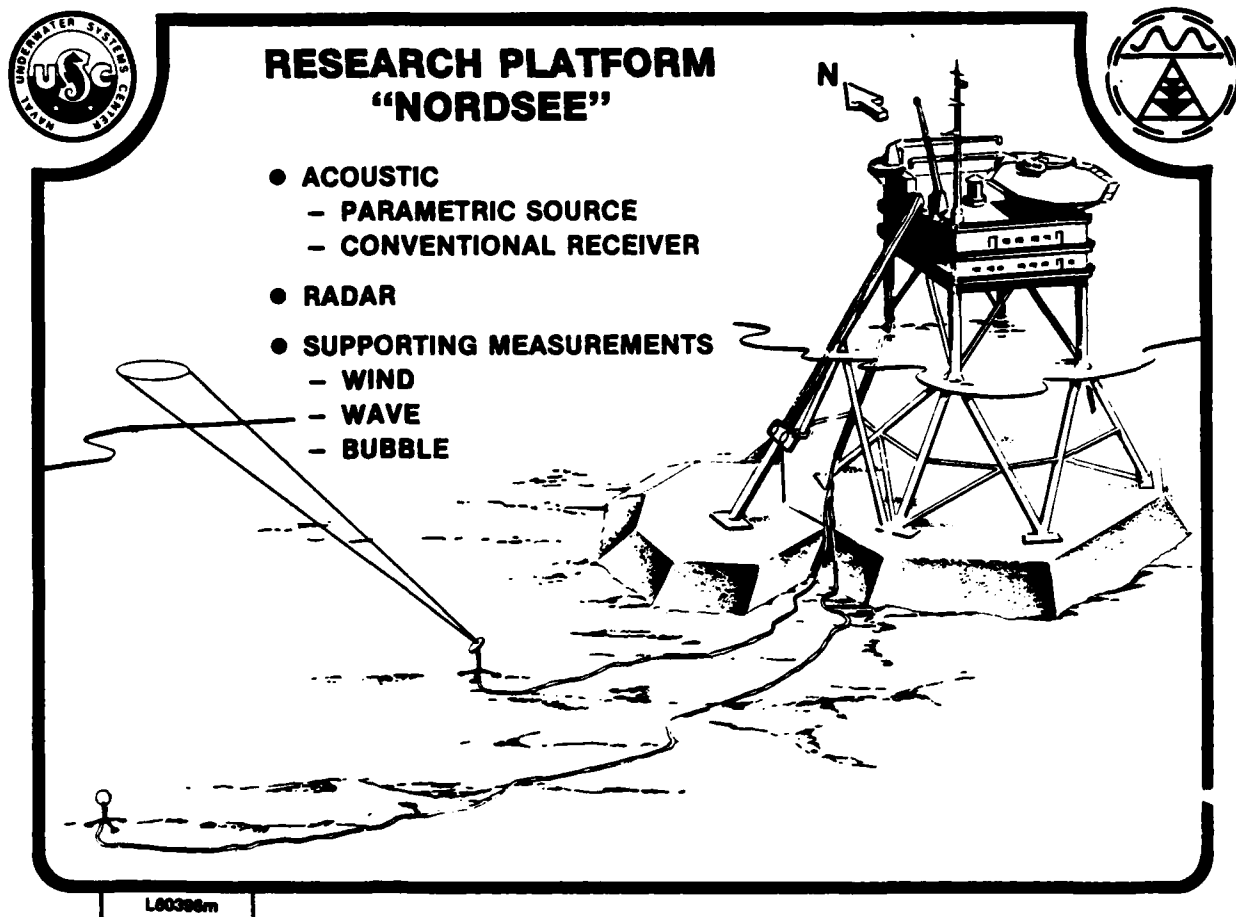
THE INFLUENCE OF BUBBLES ON SEA SURFACE BACKSCATTER MEASUREMENTS

Numerous theoretical studies and experimental programs have been instituted to investigate acoustic reverberation originating at or near the sea surface. The results of these studies indicate surface roughness and air bubbles must be considered to explain the environmental dependence of acoustic scattering on sonar engineering parameters such as frequency, grazing angle, and system design characteristics.

A principal reason for conducting a recent sea surface reverberation study was to determine the frequency regime over which different environmental parameters appear to be the governing factor.

-- First viewgraph, please. --

Accession For	
NTIS CRA&I	<input checked="" type="checkbox"/>
DTIC TAB	<input type="checkbox"/>
Unannounced	<input type="checkbox"/>
Justification	
By	
Distribution /	
Availability Codes	
Dist	Avail & d/or special
A-1	

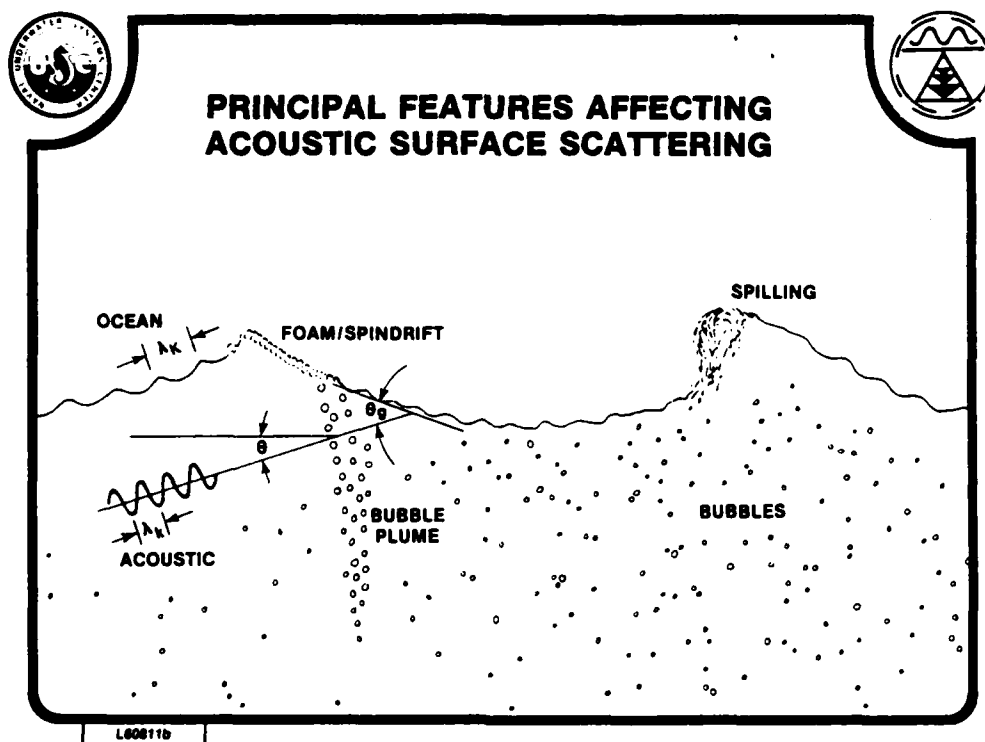


VIEWGRAPH 1

The experiment site was the Federal Republic of Germany's research platform NORDSEE, which is approximately 40 nautical miles west of the German and Danish coasts. The platform is located in approximately 30 m of water. A high resolution parametric array was installed atop a 7.5 m tower and emplaced a short distance from the platform. The parametric array was used as an acoustic projector because of its broad bandwidth, narrow beamwidths, and very low sidelobe levels, which help alleviate the problem of multipath separation. This system has a nominal 2.5 degree beamwidth at 18 kHz and could be remotely trained in elevation and azimuth. The system was also used as a conventional receiver for backscattering measurements.

In addition to these measurements, radar backscatter measurements of the sea surface were concurrently obtained. Numerous supporting measurements were also taken such as sound speed, wind velocity, subsurface bubble, and ocean wave characteristics (using photographs, video recordings, wave rider buoy, and capacitance wave staffs) [1].

-- Next viewgraph, please. --



VIEWGRAPH 2

Shown in this viewgraph are what we currently believe to be the principal features affecting acoustic surface reverberation from high resolution acoustic systems.

Based on the theoretical work of Bass and Fuks [2] a two-scale description of the sea surface is needed to characterize surface scattering. In this description, the scattering surface is represented as a superposition of short and long waves. The surface backscatter is produced by Bragg diffraction from small wavelets of wavenumber (capital K) that are equal to twice the acoustic wavenumber (small k) in the same plane. The projection into the plane is related to the grazing angle, θ_g . The large waves cause the Bragg diffraction grating to tilt, thus modifying the average grazing angle θ .

Based on the work by Thorpe and others [3, 4], bubble density in the ocean is not always horizontally stratified. When the wind is strong enough to form whitecaps, bubble clouds or plumes are generated. These plumes penetrate surprisingly far into the water column and exhibit many different characteristics similar to cloud formations in the atmosphere. The fluctuation periods of plumes are from 1 to 10 minutes.

Thus, it seems appropriate to hypothesize two types of near surface bubble formations. One consisting of uniform layers of microbubbles that form a background bubble density. The other consists of bubble plumes containing much larger bubbles of very high densities, which will exhibit temporal and spatial fluctuations as the plumes disperse and decay.

— Next viewgraph, please. —



INCOHERENT MONOSTATIC BACKSCATTER



$$I_R = I_o \sum_i \frac{\psi_i}{TLC_i^2}$$

SURFACE

$$\psi_i = \phi_i A_i$$

VOLUME

$$\psi_i = R_o V_i \sum_j N_{ij} \sigma_{ij} = R_o V_i s_{v_i}$$

COHERENT MONOSTATIC BACKSCATTER

$$I_R = \frac{I_o \phi_{coh}}{2 TLC}$$

L60811a

VIEWGRAPH 3

The intensity of an incoherently scattered acoustic wave is equal to the incident intensity times a scattering function. If we only consider monostatic backscatter and modify the incident and scattered intensity by the transmission loss, TLC, we may express the total reverberation at a receiver, I_R , in terms of intensity at the source, I_o , by the upper equation, where ψ_i is the elemental scattering cross section. We thus see the total reverberation is a sum over all contributing scattering elements.

The extent or number of scattering elements may be determined by realizing the reverberation at any instant of time is a convolution of the spatial impulse response of the scatterers and the transmitted signal [5]. When the scattering mechanisms are distributed or located such that their temporal extent is greater than the pulse length, the contributing scatterers are determined by pulse length. When the pulse length is longer than the temporal extent of the scatterers, all elemental scatterers may contribute.

Scattering cross sections are not usually presented in sonar literature. Instead the decibel measure of a scattering function related to target strength is commonly used. For scattering from a surface, the elemental scattering cross section, ψ , is simply related to the scattering function, ϕ , by the second equation, where A is an area. Surface scattering strength is $10 \log \phi$. For an admixture of air bubbles and water, the elemental scattering cross section is related to the scattering coefficient, s_v , by the

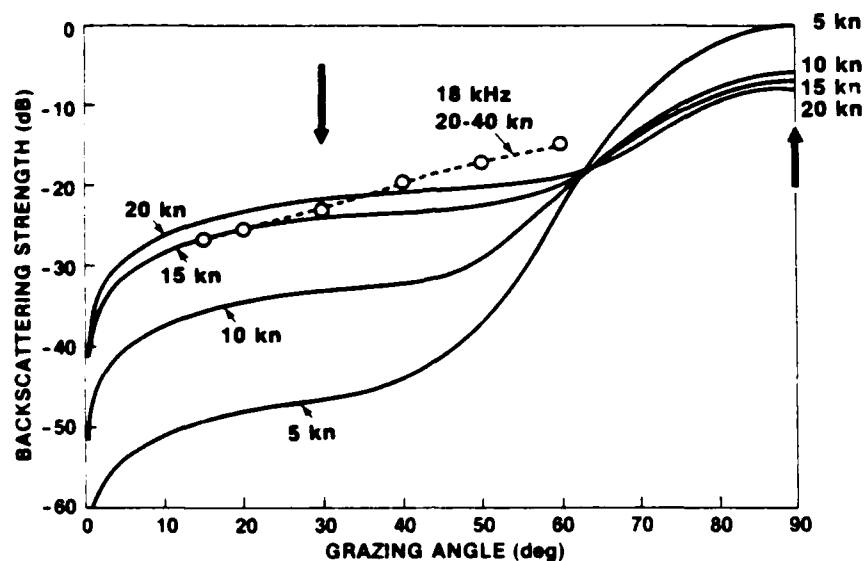
third equation. Here we should note the scattering coefficient is a sum over the number j of bubbles in the elemental volume, V_j , and depending on the distribution may not be principally controlled by resonant bubble size. In addition, σ_{ij} is the scattering cross section of a bubble and is strongly dependent on acoustic frequency near and below resonance. Volume scattering strength is $10 \log$ of the volume scattering coefficient times a reference range, normally 1 m.

The intensity of a coherently scattered acoustic wave is found by using the solution of the image reflection problem at a plane interface. For the normal incidence case, the source and receiver are colocated and the solution is given by the fourth equation. The reflection loss in this case is simply $10 \log$ of the scattering function ϕ .

-- Next viewgraph, please. --



SURFACE BACKSCATTERING STRENGTH vs GRAZING ANGLE FOR VARIOUS WIND SPEEDS



L808111

VIEWGRAPH 4

This viewgraph depicts surface backscattering strength versus grazing angle for various wind speeds. The solid lines are the result of the model recommended by the Applied Physics Laboratory at the University of Washington for use at ultrasonic frequencies [6]. The dashed lines indicate the average results of our experiments at a comparable frequency at high wind speeds as measured 47 m above the sea surface. Several results are noteworthy. First, there is good agreement between the model and the data. Secondly, we can observe that at low grazing angles backscattering strength increases with increasing wind speed but appears to reach a maximum or saturation value above 20 knots. We also note scattering strength behaves in the opposite manner at very high grazing angles. In addition, this viewgraph serves as a guide to the specific backscattering parameters we wish to address. That is the dependence of backscattering strength at the two grazing angles indicated by the arrows at 90 and 30 degrees as a function of the environment in the frequency regime of 18 to 3 kHz.

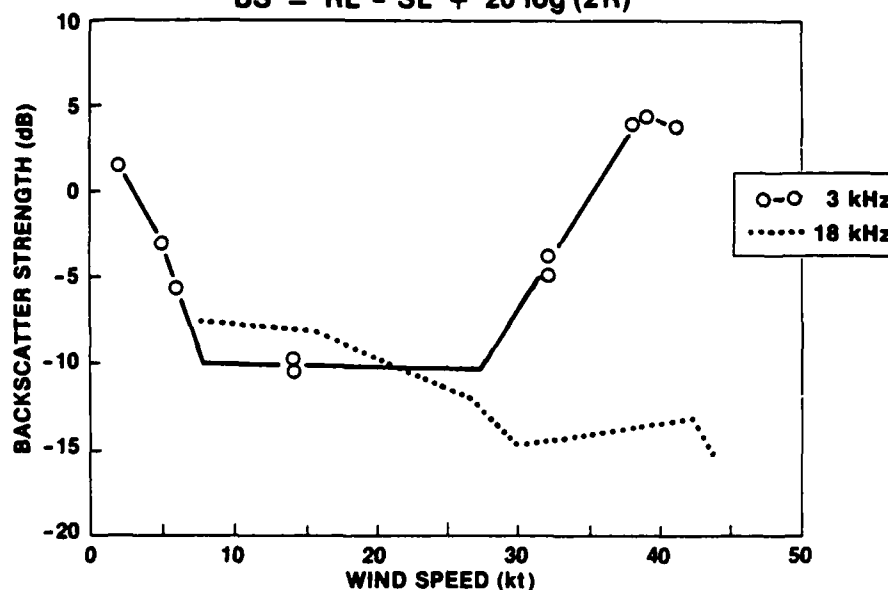
-- Next viewgraph, please. --



NORMAL INCIDENCE BACKSCATTER vs WIND SPEED



$$BS = RL - SL + 20 \log (2R)$$



L60811c

VIEWGRAPH 5

This viewgraph illustrates backscatter strength as a function of wind speed at 3 and 18 kHz for normal incidence.

Backscattering at normal incidence is considered here to be a coherent process. The backscatter strength values (BS) are corrected for source level (SL) and transmission loss only.

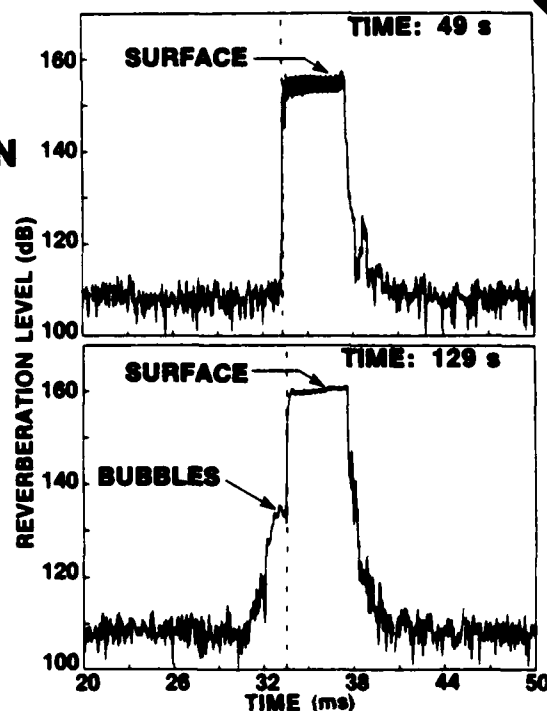
At 18 kHz it can be seen backscatter strength decreases as wind speed increases up to about 30 knots. Beyond this wind speed, it appears a saturation region is reached and there is no longer any significant correlation between backscatter and wind speed. This is the same trend predicted by the APL-Washington model and has been observed many times. The data at 3 kHz are significantly different. At very low wind speeds there is a strong dependence on wind speed. This is to be expected because in this region the Rayleigh roughness parameter is small. Had our experimental data at 18 kHz extended to comparable low wind speeds we would expect the same trend. For higher wind speeds the scattering strengths at 3 and 18 kHz are similar, until at wind speeds above 28 knots the scattering strength again shows a dependence on wind speed attaining a saturation in the 38 knot region. Though not shown here, our data at intermediate frequencies exhibit the same trend. It thus appears other phenomena must be playing a significant role in the backscattering mechanism. To examine this more carefully, individual returns obtained at 18 kHz in the saturation region were examined.

-- Next viewgraph, please.--



SINGLE PING NORMAL INCIDENCE ACOUSTIC REVERBERATION

FREQ = 18 kHz
H_{1/2} = 3.3 m
U₄₇ = 27 kt



L60398k

VIEWGRAPH 6

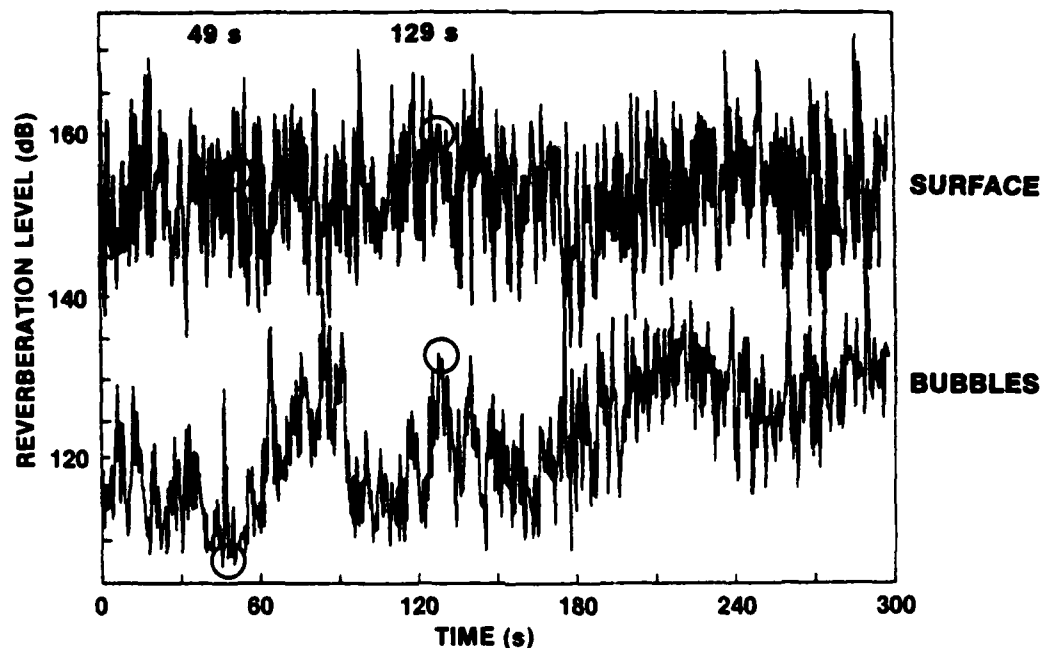
This viewgraph shows the envelope of the time series for two different pings at normal incidence. The transmitted frequency was 18 kHz with a pulse width of 4 ms. The significant wave height was 3.3 m and the wind speed was 27 knots. During this time period many breaking waves occurred. The upper plot shows a single ping return 49 s after the measurement set started. As seen from the steep slope at the beginning of the echo there is no obvious bubble reverberation. The lower plot, which shows the return from another ping 80 s later, indicates the presence of bubbles down to about 1 m below the surface. To investigate the influence of bubbles on the sea surface backscatter for normal incidence, the reverberation levels received from the surface and from the bubbles were evaluated for each individual ping. The surface reverberation levels to be presented are the average over the 4 ms past the very steep slope. The bubble reverberation level is the average over 1 ms starting 1.6 ms before this slope.

— Next viewgraph, please. —



REVERBERATION LEVEL vs TIME FROM SURFACE AND BUBBLE SCATTERERS

FREQ = 18 khz

 $H_{1/2} = 3.3$ m $U_{47} = 27$ kt

L60396h

VIEWGRAPH 7

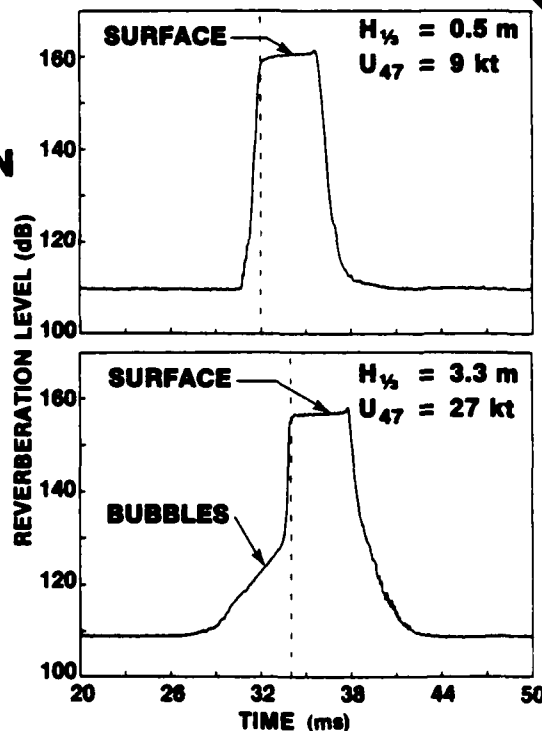
This viewgraph depicts the reverberation from the surface and the bubbles from each ping using the method just described. The circles indicate the levels that correspond to the two pulses just shown. The time series is 300 s and is a result of 750 pings at a repetition rate of 0.4 s. It can be seen that there is no correlation between surface reverberation and bubble reverberation levels. The reverberation from the surface has a relatively stationary mean. The reverberation level from the bubbles is considerably lower in amplitude and exhibits slowly varying characteristics of much longer time duration than associated with any wave components. This indicates the generation of bubble patches probably caused by breaking waves, which remain below the surface for an extended period of time. This agrees with our visual observations during the experiment.

-- Next viewgraph, please. --



ENSEMBLE AVERAGE NORMAL INCIDENCE ACOUSTIC REVERBERATION

FREQUENCY: 18 kHz
ENSEMBLE : 750



L803981

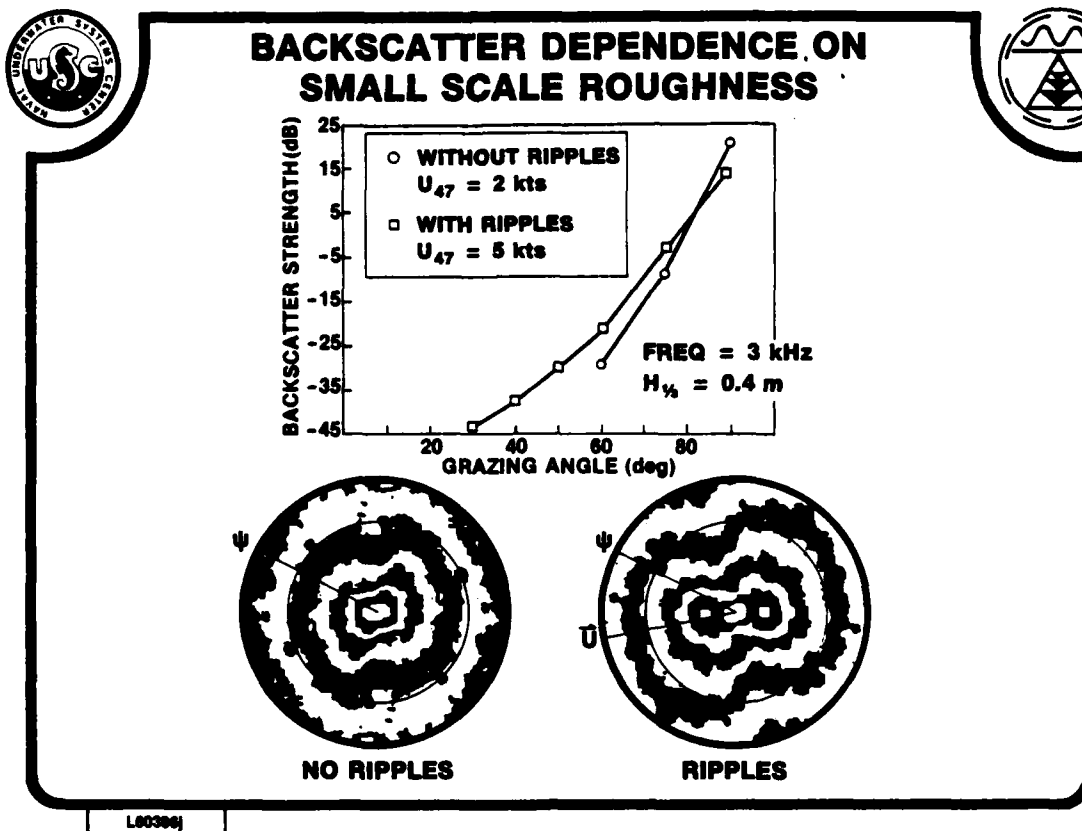
VIEWGRAPH 8

The envelopes of time series averaged over 750 pings resulting from two different environmental conditions are shown in this viewgraph.

In both cases the transmit frequency was 18 kHz. The arrival time difference of the individual echoes caused by differing wave heights was removed using a thresholding technique. The upper curve shows the average return for a wind speed of 9 knots and a significant wave height of 0.5 m. The nearly constant steep slope of the leading edge indicates there is no apparent scattered energy from a subsurface bubble layer. The lower curve is the average from a high sea state condition. The onset of scattered energy corresponds to a depth of about 3.5 m below the surface. The reverberation level increases until the difference between surface and subsurface scattered energy is about 28 dB. We may thus conclude that at normal incidence and 18 kHz bubbles are not a dominant scattering mechanism for winds up to at least 27 knots.

Using the same analysis technique for the 3 kHz data we found no precursor caused by bubbles in the averaged time series. At lower frequencies, the effects caused by bubbles are even lower at normal incidence, as expected.

-- Next viewgraph, please. --



VIEWGRAPH 9

This viewgraph illustrates the influence of wind speed on backscattering strength for the low frequency, low wind speed regime and an extended set of grazing angles.

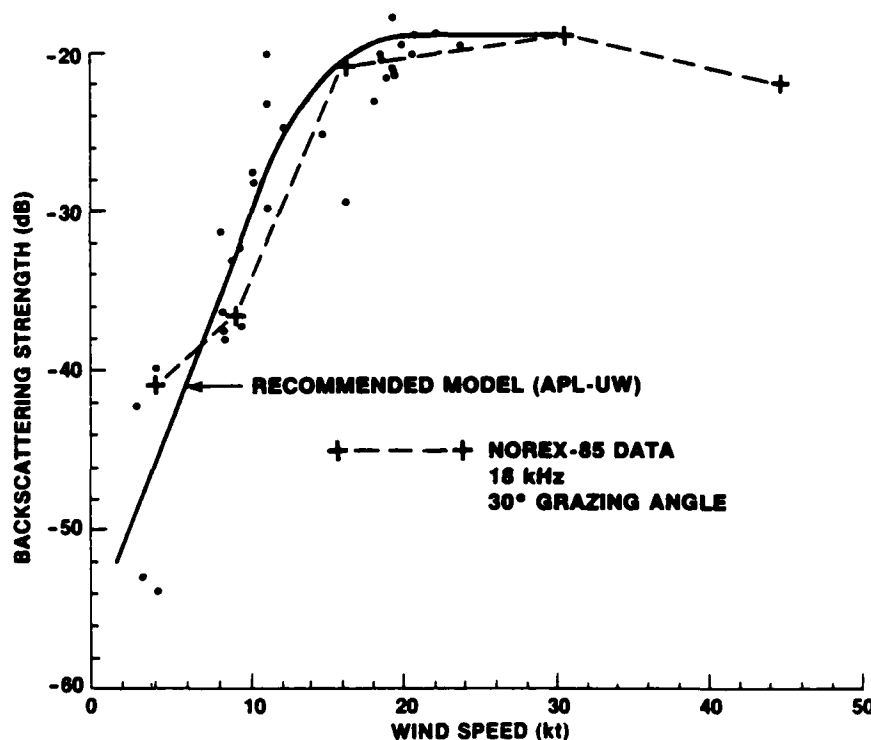
During one measurement set at 3 kHz, the wind speed increased from 2 to 5 knots. This changed the sea surface from glossy to one covered with small ripples. The significant wave height was constant at 0.4 m. The upper curves show backscattering strength as a function of grazing angle for these two conditions. At normal incidence the backscatter strength for the glossy surface is about 6 dB higher than for the case where ripples are present. For lower grazing angles, the ripples cause higher backscattering such that at 60 degrees the difference is about 8 dB. During these measurements, photographs of the sea surface were taken and analyzed using Stilwell's technique as modified by Baur [7]. The results of this analysis, shown in the lower part of the viewgraph, depict the associated directional wave spectra. The analysis bandwidth presented is from 1 to 3 Hz. The contour interval, depicted by the intersection of a black and white stripe is 6.5 dB. The vector U shows the wind direction and ψ indicates the azimuthal orientation of the acoustic axis. The inner circle is drawn for a surface wavelength of 0.25 m. This corresponds to the acoustic wavelength at 3 kHz. The energy of the waves at this frequency in the direction of the acoustic axis is about 10 dB higher when ripples are present. It is expected that the difference between the backscatter values would become greater for lower grazing angles as indicated by the different slopes of the two backscatter curves.

We may thus conclude at low wind speeds and all grazing angles backscatter at 3 kHz is strongly dependent on the high frequency ocean wavenumber spectrum.

-- Next viewgraph, please. --



WIND SPEED DEPENDENCE OF BACKSCATTERING STRENGTH

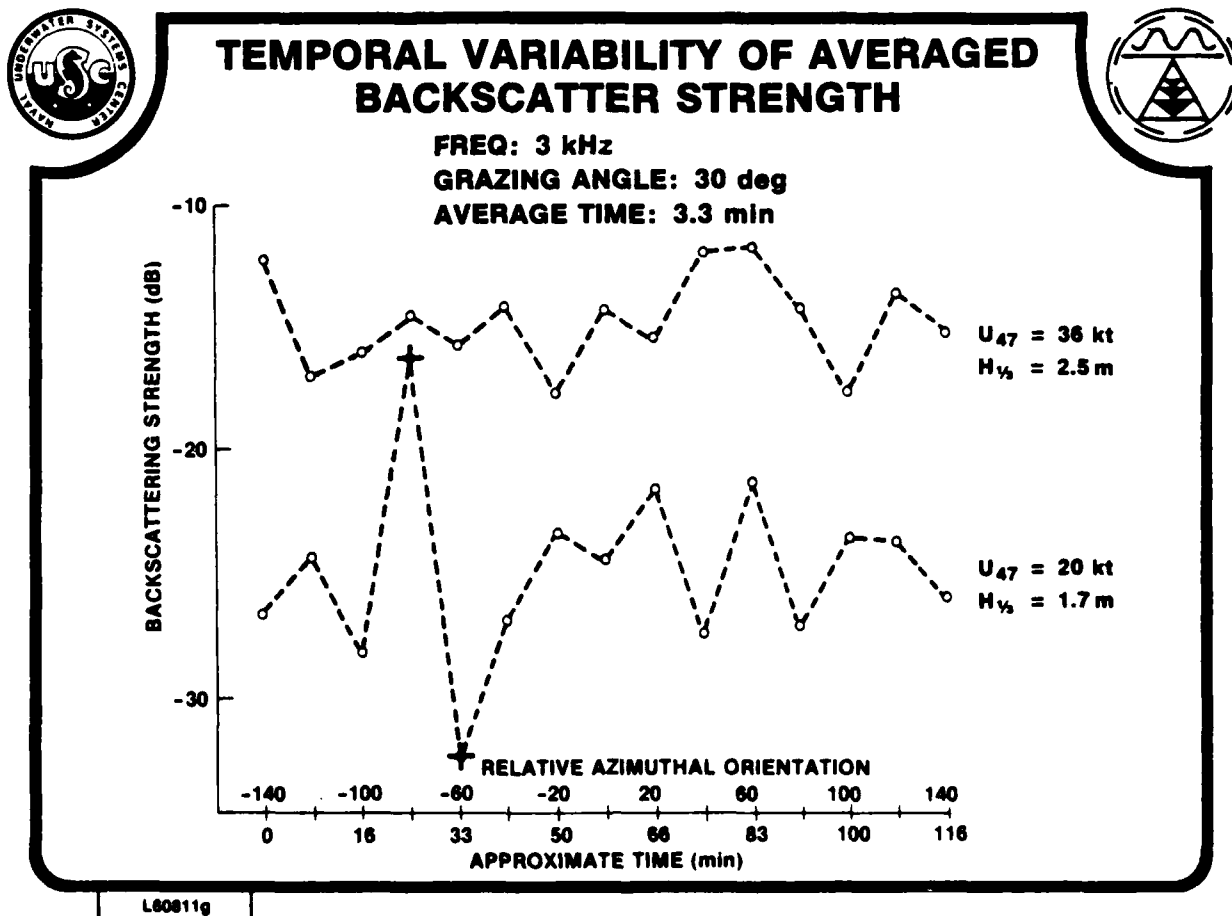


L80811e

VIEWGRAPH 10

This viewgraph illustrates the wind speed dependence of backscatter for low grazing angles near ultrasonic frequencies. The solid line represents APL-University of Washington's recommended model; the dots are a part of the data base upon which the model is founded and the dashed line is the result of our measurements. As with the previous comparison between the recent data set and APL's model, there is no significant difference between averaged results at comparable frequencies. Of concern to sonar engineers dealing with high data rates, high resolution sonars and advanced processing techniques is when one may rely on averaged results. The problem shall be illustrated for lower frequencies where the transition to the saturated region is less rapid.

-- Next viewgraph, please. --



VIEWGRAPH 11

This viewgraph represents data acquired in attempting to investigate the azimuthal dependence of backscatter relative to wave direction during two environmentally different periods. Each data point represents an average of 500 returns in a 3.3 minute period. The azimuthal transmit direction was then changed by 20 degrees and the next data set obtained. During the measurement periods of about 2 hours, the environmental conditions did not appreciably change.

We found no correlation between azimuthal transmit and wave direction for the given wind speed case, but it is apparent there is substantial variation between 3.3 minute averages. The highest difference is 16 dB for the two consecutive events marked by crosses in the lower curve.

To investigate the high degree of variability, the time history of these two events was plotted on a ping-to-ping basis.

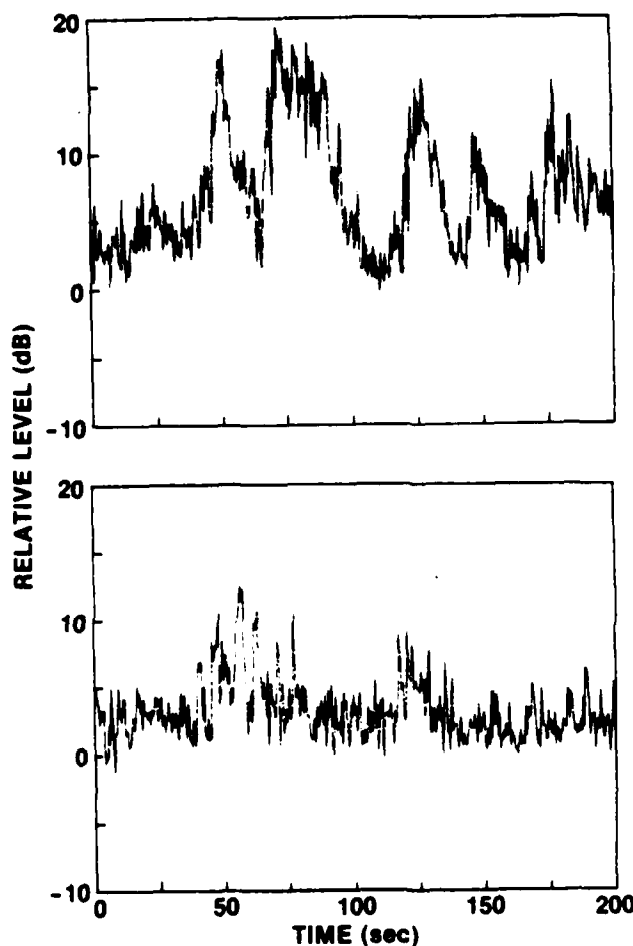
- Next viewgraph, please. --



TIME HISTORY OF BACKSCATTER ENERGY

FREQ: 3 kHz

GRAZING ANGLE: 30 deg



$H_{1/2} = 1.7 \text{ m}$
 $U_{47} = 20 \text{ kt}$
 AZIMUTH
 -80°
 $T_0 = 0$

$H_{1/2} = 1.7 \text{ m}$
 $U_{47} = 20 \text{ kt}$
 AZIMUTH
 -60°
 $T_0 = 5 \text{ min}$

L80811h

VIEWGRAPH 12

The backscattered energy from 500 pulses at a repetition rate of 0.4 s is shown in each of these figures. The instantaneous energy was obtained at the time when the average maximum backscattered energy occurred. These two time series, though obviously of different character, were obtained 5 minutes apart at the same frequency. We see the backscatter energy suddenly increases by almost 20 dB and exhibits different decay rates comparable to the fluctuation periods of bubble plumes. It is obvious the average backscatter strength is affected by these long term fluctuations, that is the magnitude and duration of the high backscatter periods.

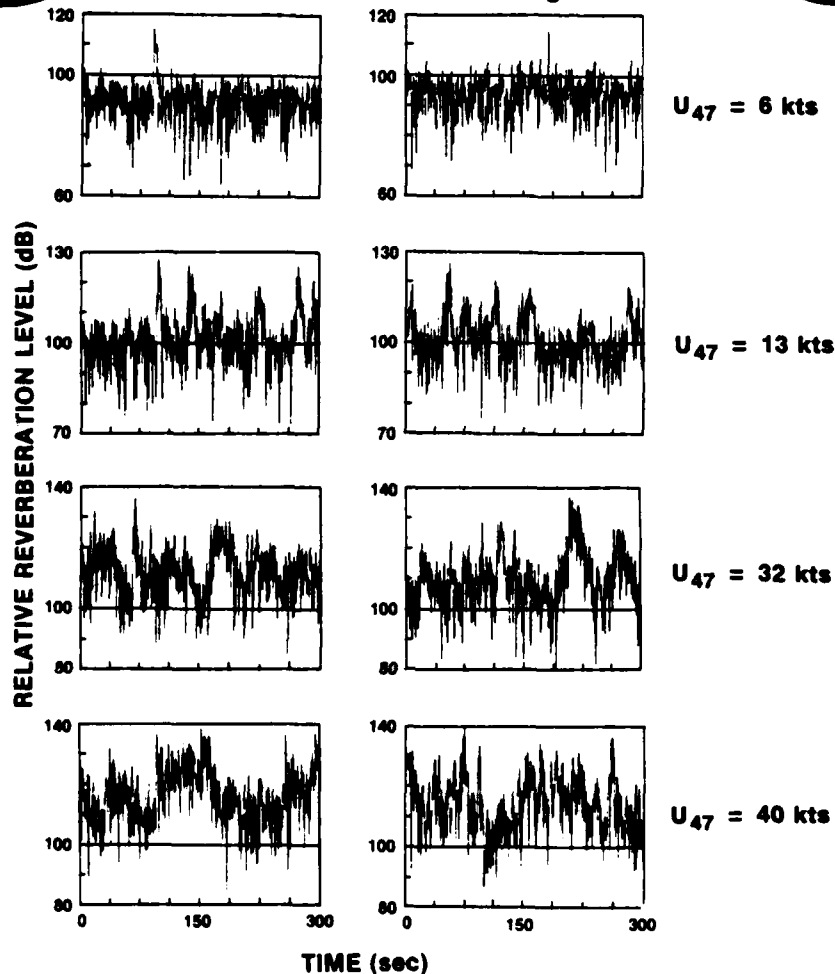
- Next viewgraph please -



TIME HISTORY OF BACKSCATTER ENERGY

FREQ: 3 kHz

GRAZING ANGLE: 30 deg



L80811d

VIEWGRAPH 13

This viewgraph illustrates in a qualitative manner the dependence of 3 kHz backscatter variability on wind speed. The solid line indicates the same level for all plots. At the lowest wind speed of 6 knots, there are almost no fluctuations. As wind speed increases, we note the high scattering periods occur more often and persist for longer periods of time. The amplitude of the high scatter periods does not, however, appear to change appreciably. Comparing the curve at 13 and 40 knots, one notes an almost inverse behavior. At the lower wind speeds, there are short periods of high scatter while at high wind speeds, the backscatter drops down for only short periods of time. At the high wind speeds, the backscatter strength remains high for periods much too long to correlate even with the longest ocean waves. We must, therefore, conclude another mechanism such as bubbles is governing backscattering even at 3 kHz.

Correlating the acoustic and bubble measurement is not possible because the bubble diameter for resonant scattering at this frequency is 2.2 mm; much too large to be measured with the optical bubble sensor used during the experiment. Bubbles of this size can only be generated by breaking waves. Video recordings were made of the acoustically insonified area during the experiments and a qualitative correlation on a ping-to-ping basis indicated reasonable agreement between breaking waves and periods of high backscatter. The correlation was particularly good when the backscattering strength increased very sharply with time.

We may, thus, conclude that for a grazing angle of 30 degrees and an acoustic frequency of 3 kHz, there is a transition from one scattering phenomenon to another. All indications lead us to believe the principal mechanism at low wind speeds is Bragg scattering from the sea surface and the principal mechanism at very high winds is volume scattering from localized bubble concentrations in the form of plumes or clouds.

We might expect bubbles to contribute to reverberation for high winds, however, the occurrence of the high scattering value shown in the upper left hand figure for winds of 6 knots is a curiosity. The video recording contained no breaking waves. A possible explanation is given by Middleton and Mellen [8]. They propose wind-generated solitons, moving nondispersively on the wind-driven drift layer are a plausible mechanism for large backscatter returns in the absence of near-surface bubble layers. Because wind stress was not measured during the experiments, we offer no further comment on this aspect of the data.

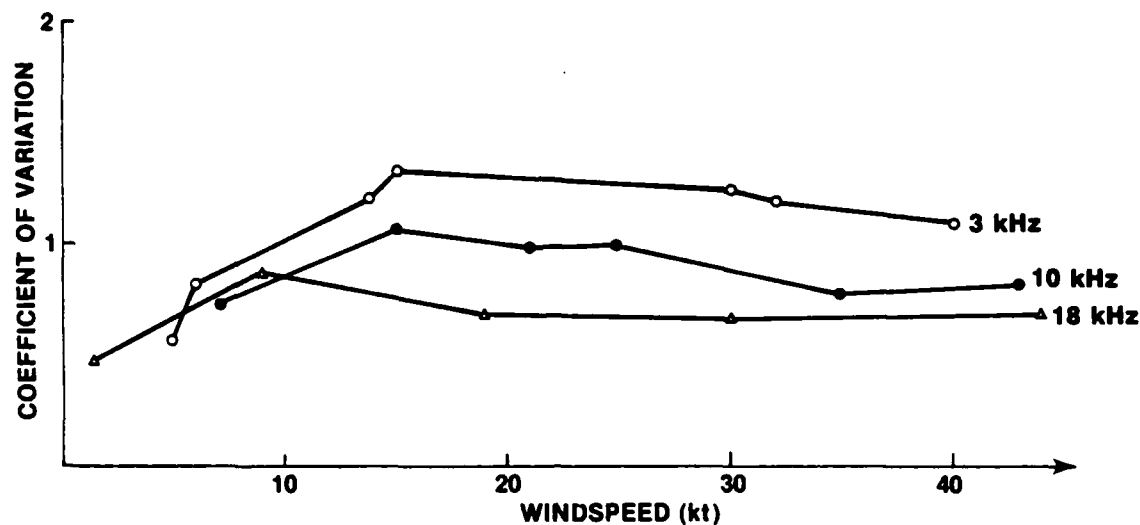
Curves obtained using the same analysis process at other frequencies exhibit the same behavior when the significant wave height is 1 m or greater.

Based on experience from previous experiments and analyses at lower wind speeds, we assumed backscattering to be a stationary process as long as the sea state remained constant. As can be seen from this viewgraph, the mean and standard deviation of the backscatter energy show strong differences when the time series is relatively short. To increase the integration time, the data from three events, obtained in temporal sequence, were combined and analyzed to obtain the normalized standard error or coefficient of variation.

-- Next viewgraph, please. --



COEFFICIENT OF VARIATION FOR 3 FREQUENCIES AS A FUNCTION OF WIND SPEED FOR A GRAZING ANGLE OF 30°



L60811J

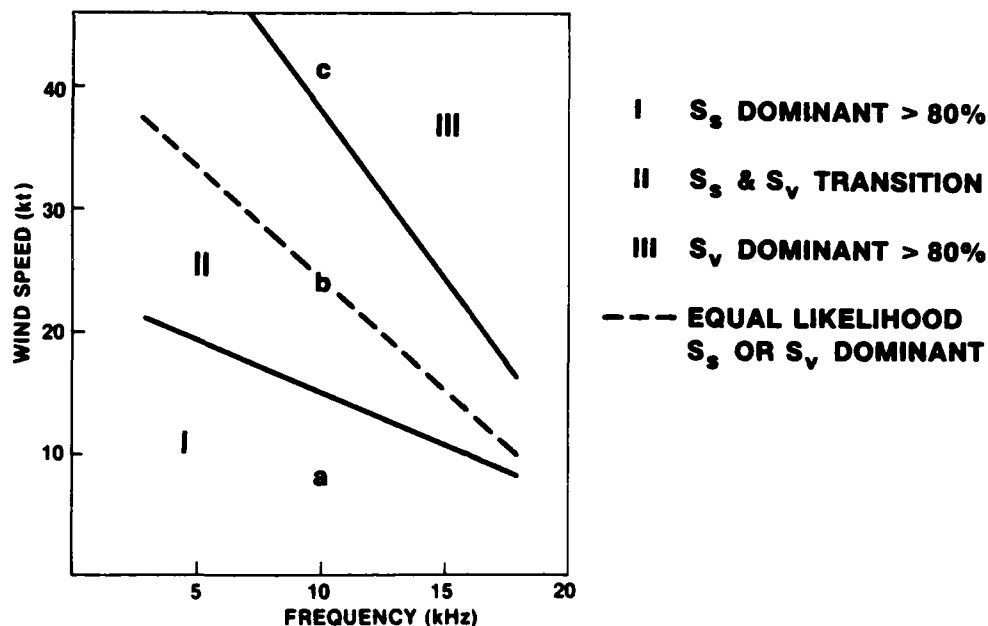
VIEWGRAPH 14

The coefficient of variation as a function of wind speed for three frequencies is shown in this viewgraph. This coefficient provides a normalized measure of variance. The envelope of a scattered signal from a surface with Gaussian distributed wave heights should exhibit Rayleigh characteristics. The coefficient of variation for a Rayleigh process is 0.52. We see in this viewgraph at the very low wind speeds the coefficient is near this value at all frequencies. The coefficient then increases with wind speed. The wind speed at which this increase stops is strongly frequency dependent. At 18 kHz, this value is about 10 knots. Beyond that the coefficient decreases to a new plateau at about 18 knots. At still higher wind speeds, the coefficient is nearly constant. Recall this is the same wind speed at which backscatter strength reaches a saturation value. It, thus, appears scattering for this situation is the result of two random processes of different amplitude. One which we attribute to Bragg scatter dominating at very low wind speeds. The second, which we attribute to near surface bubble plumes, dominating at wind speeds above 18 knots. The two are in maximum competition at about 10 knots. A similar analysis can be done at the other frequencies. At 10 kHz it appears maximum competition at about 15 knots and bubble plumes dominating in the 35 knot region. At 3 kHz the data are somewhat sparse but the maximum competition is in the 20 knot region and bubbles never seem to completely dominant even with 40 knot winds.

-- Next viewgraph, please. --



SCATTERING MECHANISM CONTRIBUTION AS A FUNCTION OF WIND SPEED AND FREQUENCY AT 30° GRAZING ANGLE



L808111

VIEWGRAPH 15

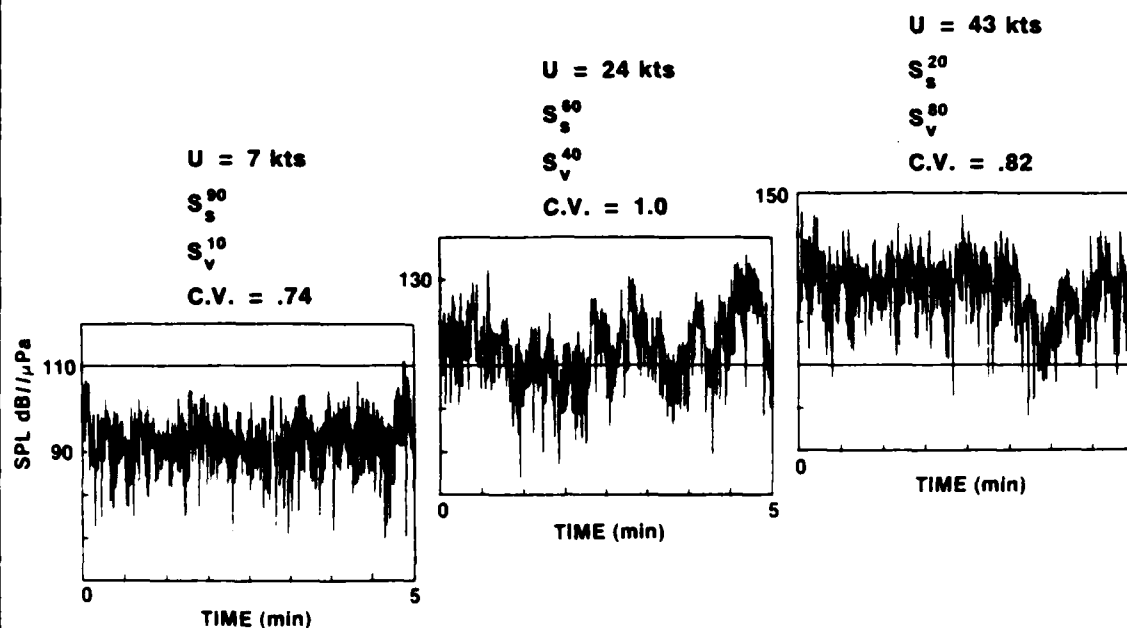
In an attempt to determine the frequency and environmental regimes over which one or the other mechanism is dominant at 30 degrees a subjective analysis of each time series was made to determine the relative period of time each mechanism appeared to be dominating the total scattering strength. This viewgraph, which is a result of that analysis contains three regions. Region I corresponds to frequencies and wind speeds in which surface scattering is the dominant mechanism at least 80% of the time. Region II is a transition region with the dashed line corresponding to equal time periods of surface and bubble scattering. Region III corresponds to frequencies and wind speeds in which volume scattering from near surface bubbles is the dominant mechanism at least 80% of the time.

The dominating mechanism is very dependent on grazing angle and as indicated earlier a similar figure at 90 degrees would only contain region I. Note the locations of the letter a, b, c. They correspond to three different regimes at 10 kHz.

-- Next viewgraph, please. --



TEMPORAL VARIABILITY OF BACKSCATTER AT 10 kHz FOR A 30° GRAZING ANGLE AT 3 WIND SPEEDS



L60811k

VIEWGRAPH 16

Because the method used to determine relative time periods is subjective three samples of each time series corresponding to letters a, b, and c are shown in this viewgraph. The left time series corresponds to low wind speed where only two short periods near the beginning and end of the file contain high values of backscatter. In this case an estimate that 90% of the time reverberation was the result of surface scattering was made. The opposite extreme for 10 kHz is shown at the right. Here the wind speed is 43 knots and relatively high values of backscatter are present about 80% of the time. The middle plot illustrates the case when both surface and bubbles contributed to scattering for region II.

— Next viewgraph, please. —



CONCLUSIONS



THE RELATIVE CONTRIBUTION OF DIFFERENT BACKSCATTERING MECHANISMS IS DEPENDENT ON WIND SPEED, GRAZING ANGLE AND FREQUENCY. THE WIND SPEED DEPENDENCE CAN BE DESCRIBED BY THREE REGIONS:

REGION I (LOW WIND SPEEDS)

- SCATTERING IS CAUSED BY BRAGG DIFFRACTION
- STRONG DEPENDENCE OF SCATTERING ON THE HIGH FREQUENCY OCEAN WAVENUMBER SPECTRUM AT ALL GRAZING ANGLES
- LOW TEMPORAL VARIABILITY

REGION II (INTERMEDIATE WIND SPEEDS)

- SCATTERING IS CAUSED BY THE SEA SURFACE AND SUB-SURFACE BUBBLES
- STRONG FLUCTUATIONS OF BACKSCATTERING WITH TARGET-LIKE RETURNS

REGION III (HIGH WIND SPEEDS)

- SCATTERING IS CAUSED BY BUBBLES
- SATURATION OCCURS WHICH IS FREQUENCY AND GRAZING ANGLE DEPENDENT
- LOW TEMPORAL VARIABILITY

L608111

VIEWGRAPH 17

In conclusion, the relative contribution of different backscattering mechanisms is dependent on wind speed, grazing angle, and frequency. The wind speed dependence can be described by three regimes.

In region I, at low wind speeds, the scattering is caused by Bragg diffraction. Here, we see a strong dependence of scattering on the high frequency ocean wavenumber, spectrum at all grazing angles. The time history of backscattering shows low temporal variability.

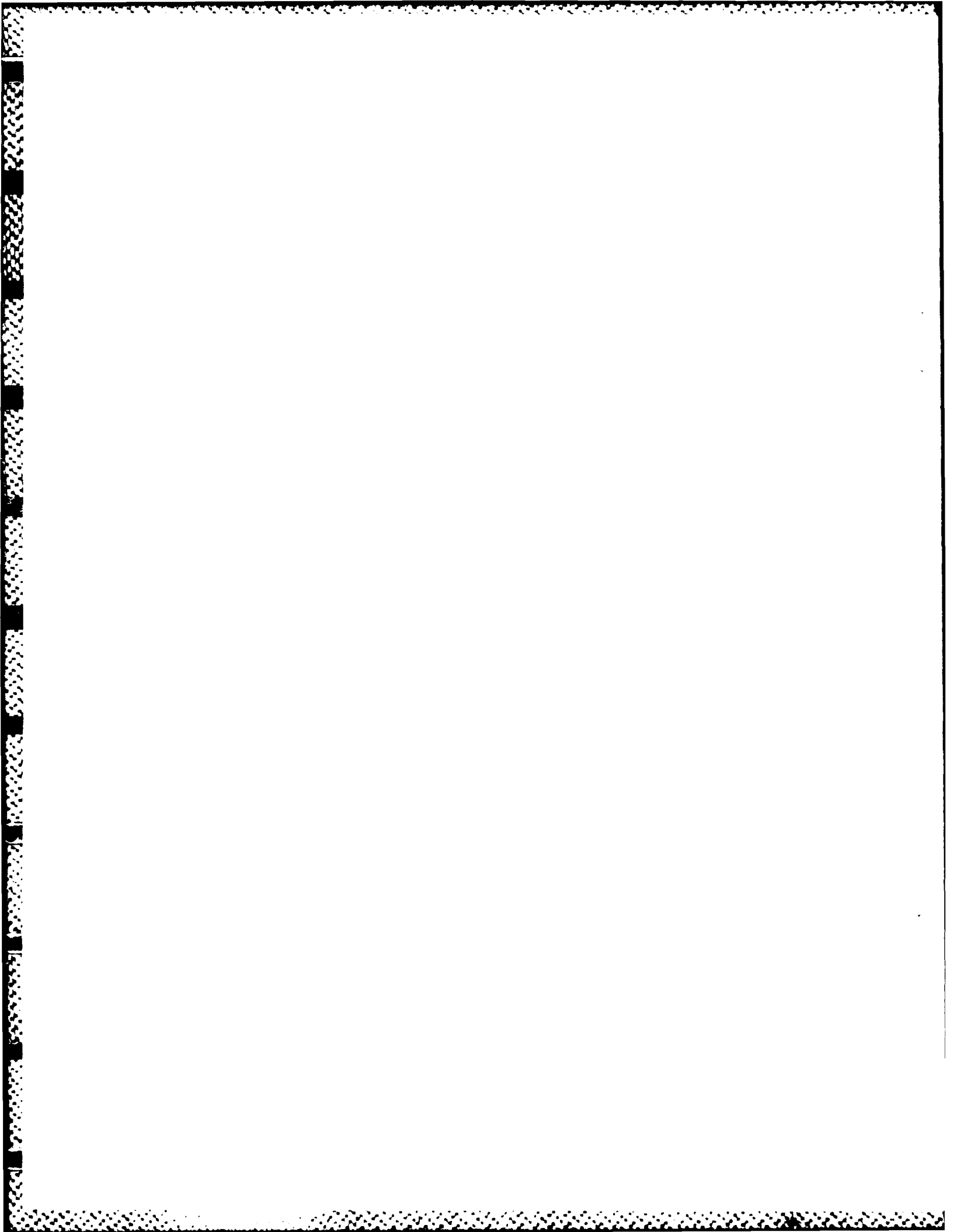
In region II, at intermediate wind speeds, the scattering is caused by the sea surface and subsurface bubbles. The time history of backscattering shows strong fluctuations with target-like returns.

In region III, at high wind speeds, the scattering is caused by bubbles. In this regime, saturation occurs which is frequency and grazing angle dependent. The temporal variability of backscattering decreases again.

Thank you. Are there any questions?

LIST OF REFERENCES

1. B. Nuetzel, H. Herwig, J. Monti, and P. Koenigs, A Further Investigation of Acoustic Scattering From the Sea Surface, NUSC Technical Document 7685 (FWG-Bericht 1986-3), Naval Underwater Systems Center, New London, CT, 9 July 1986.
2. F. Bass and I. Fuks, Wave Scattering From Statistically Rough Surfaces, Pergamon, New York, NY, 1979.
3. S. Thorpe, "On the Clouds of Bubbles Formed by Breaking-Waves in Deep Water, and Their Role in Air-Sea Gas Transfer," Philosophical Transactions of the Royal Society of London, A304, 1982, pp. 155-210.
4. S. Thorpe and P. Humphries, "Bubbles and Breaking Waves, Nature, vol. 283, no. 5746, 31 January 1980, pp. 463-465.
5. P. Koenigs, Transient Response of Multidimensional Arrays, NUSC Technical Report 7193, Naval Underwater Systems Center, New London, CT, 26 June 1984.
6. S. McConnell, "Formatting Strategy for NAVOCEANO Acoustic Survey Data," Applied Physics Laboratory, University of Washington, TM 2-86, 1986.
7. H. Baur, Digital berechnete STILWELLSche Richtungsspektren des Seegangs im Vergleich mit Daten oberflächengebundener Messungen, FWG-Bericht, 1980-19.
8. D. Middleton and R. Mellen, "Wind-Generated Solitons: A Potentially Significant Mechanism in Ocean Surface Wave Generation and Surface Scattering," IEEE Journal of Oceanic Engineering, vol. OE10, no. 4, October 1985, pp. 471-476.



INITIAL DISTRIBUTION LIST

Addressee	No. of Copies
NAVOCEANO	1
NAVAIRDEVCE	3
NAVCOASTSYSLAB	1
NAVPGSCOL (Library, Suk Wang Yoon, H. Medwin)	3
Marine Physical Lab, Scripps	1
Woods Hole Oceanographic Institution	1
FWG (G. Ziehm, P. Wille, W. Schmid, H. Baur, H. Herwig (5), B. Nützel (5), Bibliothek (16)	30
NORDA (Code 113, R. Farwell; 240; 241; 243; 245; 260; 270, E. Chaika, B. Blumenthal; 331, M. Su (4))	12
SACLANTCTR (Tech. Director; J. Marchment; E. Sullivan; R. Martin; Library (2))	6
OCNR (OCNR-122, 1221, 1245, 131T, 132, 231, 234, 2411)	8
ARL/PSU (S. McDaniel, D. McCammon)	2
APL/UW (C. Sienkiewicz, S. McConnell, E. Thorsos)	3
ARL/UT (H. Bocheme)	1
NOAA/NFC (F. Steimle)	1
NOSC (B. Smith)	1
NRL (E. Franchi)	1
University of Illinois (V. Twersky)	1
University of Rhode Island (P. Stepanishen, L. LeBlanc, F. Middleton, M. Wimbush, R. Watts)	5
PSI Marine Sciences (R. Mellen)	1
Defense Research Establishment Pacific (D. Thomson)	1
Institute of Oceanographic Sciences (S. A. Thorpe)	1
Raytheon Co. Submarine Signal Div. (P. Bilazarian)	1
Ferranti O.R.E. Inc. (F. C. Lowell, Jr.)	1
EDO Corp., Western Div. (R. A. Lapentina)	1
University of Miami/RSMAS (H. de Ferrari)	1
DTIC	12

END

2-87.

DTIC